Hippocampal neural stem cells rapidly change their metabolic profile during neuronal differentiation in cell culture

Martina Hruzova, Nicola Zamboni, Sebastian Jessberger
Brain Research Institute; ETH Zurich, Institute of Molecular Systems Biology;

Correspondence
jessberger@hifo.uzh.ch

Disciplines
Cell Biology
Neuroscience

Keywords
Stem Cells
Neurogenesis
Metabolism

Type of Observation
Standalone

Type of Link
Resources / Big Data

Submitted Feb 10, 2016
Published Apr 21, 2016

Triple Blind Peer Review
The handling editor, the reviewers, and the authors are all blinded during the review process.

Full Open Access
Supported by the Velux Foundation, the University of Zurich, and the EPFL School of Life Sciences.

Abstract
Throughout life, neural stem/progenitor cells (NSPCs) produce new neurons in distinct regions of the mammalian brain, a process called adult neurogenesis. Hippocampal NSPCs undergo several developmental steps until they reach their final stage of fully differentiated neuronal progeny. Failing any of those steps can compromise adult neurogenesis, resulting in impaired function of the mammalian hippocampal circuit. Altered neurogenesis has been associated with impaired learning and memory as well as a number of neuropsychiatric diseases. Previously it was shown that metabolism changes markedly between NSPCs and their differentiated progeny. However, the dynamics of metabolic adaptations (gradual vs. acute) occurring during neuronal differentiation have yet to be identified. To answer this question, we here determined the metabolic profile of mouse hippocampal NSPCs and their neuronally differentiating progeny in vitro by mass spectrometry, using an inducible differentiation system, allowing for high temporal resolution of the differentiation process. The metabolomics data we have generated show major and rather quick metabolic adaptations occurring during the first days of neuronal differentiation. Thus, we here observe that NSPCs and their neuronal progeny show distinct metabolic profiles that can rapidly change depending on their developmental state.

Introduction
In the last 50 years, it has been established that the neurogenic capacity of mammalian brain is not depleted postnatally but is being preserved throughout adult life in distinct brain regions, among them the hippocampal dentate gyrus (DG) [1] [2] [3]. Adult neurogenesis is dynamically regulated, and altered neurogenesis has been associated with a number of neuropsychiatric diseases such as major depression, aging, and epilepsy, demonstrating its importance for flawless adult brain function [4] [5] [6] [7]. Recently, it has been shown that metabolism is an important regulator of NSPCs development: it was found that NSPC require fatty acid synthase (FASN)-dependent de novo lipogenesis for proper proliferation within adult DG [8] [9]. Metabolism provides cells with energy and building blocks necessary to produce more complex molecules, therefore having a pivotal role in cell survival and proper cell function [10] [11] [12]. In addition, to a specialized lipid metabolism in NSPCs, for various other somatic stem cells such as long-term hematopoietic stem cells (LT-HSCs) and mesenchymal stem cells (MSCs), metabolism plays an important role in maintaining the stem cell pool (active anabolic pathways) or when differentiated into various tissue-specific cell types (active catabolic pathways) [13] [11] [14] [15].
However, the metabolic changes that occur during distinct developmental steps in the course of NSPC proliferation towards neuronal differentiation remain poorly described. Therefore, we here aimed to characterize the exact timing of metabolic adaptations during NSPC development using precise mass spectrometry (MS)-based metabolomics. With this approach, we observed a rapid metabolic switch from proliferating NSPCs once they enter programs of neuronal differentiation.

Objective
The objective is to define the metabolic profile of mouse hippocampal NSPCs and their neuronally differentiating progeny in vitro by mass spectrometry.

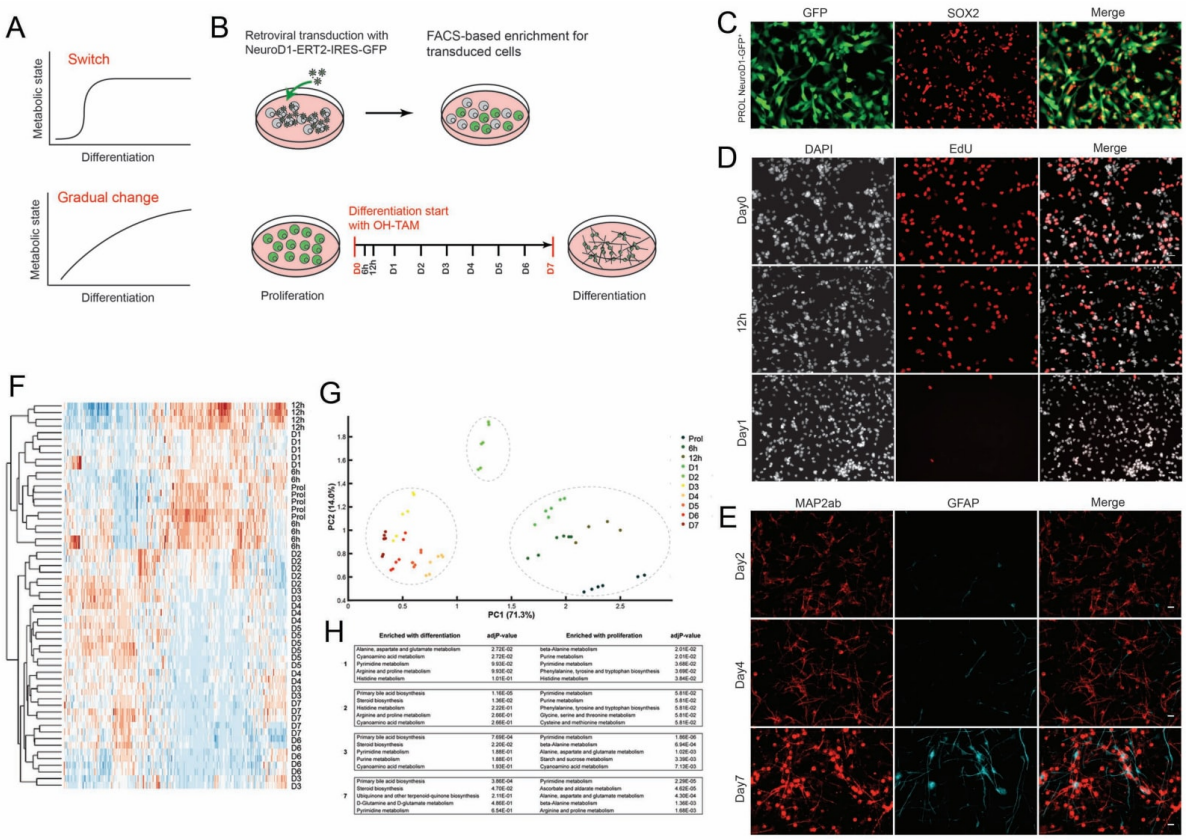

a

Figure Legend

Figure 1. Metabolic adaptations in the course of NSPC-based neuronal differentiation.

(A) In this study, we aimed to address the exact timing of metabolic changes during NSPC-based neuronal differentiation. Specifically, we asked if metabolism is changed quickly at the beginning of neuronal differentiation or gradually throughout the entire differentiation process.

(B) Experimental scheme showing the NeuroD1-induced neuronal differentiation protocol.

(C) Proliferating NeuroD1-GFP+ NSPCs (green) co-express the NSPC marker SOX2 (red).

(D) The proliferation rate 12 and 24 h (D1) after the differentiation start was analyzed using an EdU (grey)/DAPI (blue) assay.

(E) NSPC-derived progeny was analyzed for co-expression with the neuronal marker MAP2ab (red) and the glial marker GFAP (blue). Scale bars represent 20 µm.

(F) Metabolomics data analyses showing a clustered heat map of differentiating NSPCs. A clear metabolic switch can be seen between proliferating NSPCs (D0) and fully differentiated neurons (D7). Proliferating NSPCs and early differentiated neurons (D0–D1) strongly cluster together, as well as differentiating neurons from day 2 (D2) till day 7 (D7). Blue and red indicate z-scores. Red= relatively higher levels, blue= relatively lower levels (for the same ion over all samples).

(G) Principal component analysis (PCA) with two principal components for 10 different time points during neuronal differentiation. The biggest metabolic differences can be seen between day 1 (D1) and day 2 (D2) and between day 2 (D2) and day 3 (D3). From D3 to D7, the probes cluster together, showing that metabolic changes here are rather small.

(H) Metabolite enrichment analysis for 4 selected time points during NSPC differentiation (D1, D2, D3, D7) compared to D0. Shown are the top 5 (corresponding to adjusted *p*-values) metabolic pathways enriched with differentiation and proliferation, respectively.

Virus production

Retroviruses were produced as previously described [18]. In summary, the Lipofectamine 2000 kit (Invitrogen) was used to transfect human embryonic kidney cells (HEK 293T) with retroviral constructs. The virus was collected 2 days after transfection by filtering the supernatant through 0.22 µm filter top and subsequent centrifugation at 19'4000 rpm/4℃ for 2 h. Viral pellet was resuspended with 4 ml PBS and spun down with 20% sucrose cushion at 20,500 rpm/4℃ for 2 h. The final viral pellet was resuspended in 40 µl PBS.

Cell culture

Wild-type (wt) mouse hippocampal NSPCs were isolated from adult mice (6–8 weeks old) as previously described [26]. Proliferating NSPCs were cultured as a monolayer with 37℃/5% CO_2 in DMEM/F-12 (Glutamax) media supplemented with N_2 (Invitrogen), antibiotics (penicillin-streptomycin-fungizone; Invitrogen), Heparin (5 µg/ml; Sigma), human EGF (20 ng/ml; PeproTech) and human basic FGF-2 (20 ng/ml; PeproTech). Media was changed every 2 days. For neuronal differentiation, media without growth factors was used (DMEM/F-12, N_2, PSF, and heparin). For the viral infection, approximately 50,000 wt adult hippocampal NSPCs were plated on coated Poly-L-ornithine (10 µg/ml; Sigma) and Laminin (5 µg/ml; Invitrogen) 12 well plates in proliferation medium. 24 h after plating, cells were infected with 1–2 µl NeuroD1-ERT2-IRES-GFP retrovirus.

FACS

NeuroD1-ERT2-IRES-GFP virus-infected NSPCs were spun down at 300 *g* for 5 min and the cell pellet was trypsinized using 0.05% trypsin in Versene for 5 min at 37℃. Afterwards a double volume of ovumucoid trypsin inhibitor mix was added for 5 min at room temperature. Cells were resuspended with 5 ml of media and spun down at 120 *g* for 5 min. Final cell pellet was resuspended in 1 ml 1 mM EDTA in PBS or DPBS and stored on ice prior to sorting. FACS for NeuroD1-ERT2-IRES-GFP+ (NeuroD1-GFP+) cells was performed using the BD FACS Aria III Cell Sorter. For negative control/background autofluorescence, wild-type hippocampal NSPCs were used.

NeuroD1-induced neuronal differentiation

NeuroD1-induced neuronal differentiation was optimized from a previously established protocol to enable in vitro differentiation of pure neuronal cultures [18]. Proliferating NeuroD1ERT2-expressing GFP+ cells were trypsinized as described before and in parallel plated on coated (Poly-L-Lysine, 10 µg/ml and LAM) 6 well plates for metabolome analysis (330,000 cells/well in triplicates) and on coated 12 well plates (130,000 cells/well in triplicates) for the corresponding immunocytochemistry analyses. 2 days after cell plating, proliferating media was replaced with differentiating media (no growth factors) and 0.5 µM OH-TAM (Sigma; dissolved in 100% EtOH) was added. Addition of OH-TAM was defined as differentiation start (D0). Differentiation media was exchanged after 3 days. Cells were collected for metabolite extraction or in parallel for immunocytochemistry after the following time points: 6 h, 12 h, 1 day (D1), 2 days (D2), 3 days (D3), 4 days (D4), 5 days (D5), 6 days (D6) and 7 days (D7). To measure the proliferation rate during neuronal differentiation, cells on 12 well plates were pulsed with 10 mM EdU (Clik-it EdU Imaging kit; Life Technologies) for 1 h at 37℃ prior to fixation.

Immunocytochemistry

At every given time point, cells were fixed with pre-warmed (37℃) 4% paraformaldehyde (PFA) for 15 min at room temperature. Fixed plates were stored in PBS at 4℃ until immunocytochemistry was performed. Cells were treated with blocking and permeabilization buffer containing 3% donkey serum and 0.25% Triton X-100 in TBS for 30 min at room temperature. Cells were incubated with primary antibodies in blocking/permeabilization buffer overnight at 4℃. The following primary antibodies were used: goat α-SOX2 (1:200; Santa Cruz Biotechnology), rabbit α-GFAP (1:500; DAKO), mouse α-MAP2ab (1:500; Sigma). All secondary antibodies were applied for 1.5 h at room temperature in blocking/permeabilization buffer with the dilution 1:250 (Jackson Laboratories). Cell nuclei were detected with 4-6-diamidino-2-phenylindole (DAPI,

1:5000; Sigma). To analyze the cell proliferation rate, Click-it EdU Imaging kit was used according to the manufacturer's instructions.

Image analysis

Images were taken on a Zeiss Observer Z1 microscope. To analyze proliferation rate 12 h and 1 day (D1) after differentiation start, we quantified EdU and DAPI-stained nuclei. Both stained nuclei were automatically counted by self-written Fiji macro program. Number of EdU-positive DAPI nuclei was compared to EdU-negative DAPI nuclei to calculate the proliferation rate. Statistical analysis was performed using Prism6. Ordinary one way ANOVA test was performed, followed by Turkey's multiple comparisons test, p <0.0001, n= 3, SEM shown.

Quantification of neuronal and astroglial progeny with and without NeuroD1 induction

We plated 60,000 NeuroD1-GFP+ hippocampal NSPCs cells/well for each condition on glass coverslips coated with Poly-L-ornithine (50 µg/ml) and LAM (5 µg/ml) in proliferating media (DMEM/F-12 supplemented with N_2, heparin and growth factors as previously described). After 24 h, we changed the media to differentiation media (DMEM/F-12 supplemented with N_2, heparin but no growth factors) and cells were treated either with EtOH or OH-TAM (0.5 µM; SIGMA) for 2 days. During the whole differentiation process, cells were kept in differentiation media. After 7 days of differentiation, cells were fixed and stained with DAPI, anti-MAP2ab and anti-GFAP antibodies as previously described. Confocal images were taken on Olympus microscope. 5 images per well were taken. To quantify the amount of cells expressing MAP2ab and GFAP markers, we used self-written FiJi macro: a Z-stack was created with MAX intensity for all images. First, we counted DAPI particles by using the following functions: find edges, make binary, fill holes, watershed and analyze particles size 30–300, circularity 0.40–1.00. Then we analyzed MAP2ab and GFAP expression by setting a threshold and converting it to a mask. Threshold was adjusted for each condition to yield a better separation of MAP2ab and GFAP-positive cells and to eliminate any overlap in the channels. This mask was selected and laid over the DAPI particles. Then all DAPI particles overlaying the GFAP or MAP2ab mask were counted using the analyze particle function with size 30–300, circularity 0.30–1.00. The counted particles for MAP2ab and GFAP were divided by the DAPI counted particles to get the ratio of MAP2ab and GFAP-positive cells per condition. In total, 3,197 DAPI+ cells were counted for ETOH condition and 2249 DAPI+ for OH-TAM condition.

Metabolite extraction

At every given time point, cells were washed with 75 mM ammonium carbonate (Sigma) pH 7.4 and snap-frozen on the plates with liquid nitrogen. Metabolites were extracted by treating the snap-frozen plates with hot extraction solution (70% EtOH) on heating block (75℃). The plate was re-extracted with hot extraction solution 2 more times, allowing for a high recovery rate. Note that the extraction efficiency is irrelevant for the analyses performed here given that we did not perform quantitative analyses but a qualitative comparison between conditions. Hence, full recovery is not a precondition to detect difference in metabolites across groups. Supernatant containing metabolites from all 3 extractions was pooled, spun down, and stored at -80℃ until mass spectrometry measurements.

Mass spectrometry measurements and data analyses

For non-targeted metabolite profiling, metabolite samples were analyzed by flow injection analysis on an FIA Agilent Q-TOF 6550 QTOF instrument (Agilent, Santa Clara, CA) in negative mode at 4 GHz, high resolution in a m/z range of 50–1000 [27]. A 60:40 mixture of isopropanol:water supplemented with NH_4F at pH 9.0, as well as 10 nM hexakis (1H, 1H, 3H-tetrafluoropropoxy) phosphazine and 80 nM taurochloric acid for online mass calibration. Ions were putatively annotated to metabolites based on exact mass using a tolerance of 0.001 Da and the KEGG hsa database following the procedure described in [27]. Notably, this procedure does not allow distinguishing metabolites with same molecular formula or weight. For full disclosure, all putative matches are reported in Table S1. All data analyses were performed using Matlab (The Mathworks, Natick).

Results & Discussion

Since it has been shown that NSPCs change their metabolism during their development [9], we analyzed metabolic changes in the course of NSPC-based neuronal differentiation to address the question if cellular metabolism changes gradually or rather acutely (Fig. 1A). To induce neuronal differentiation of NSPCs isolated from the adult murine hippocampus, we used retroviruses expressing the transcription factor NeuroD1 fused to a tamoxifen (TAM)-regulatable estrogen receptor (ERT2) [16] [17] [18]. With this approach, the functional expression of NeuroD1 can be tightly controlled by the addition of TAM, allowing for studying the metabolome of differentiating neurons with high temporal resolution. In contrast to standard in vitro differentiating conditions (i.e., withdrawal of growth factors) that result in mixed populations of only 20–30% neurons and a majority of astroglial cells, the NeuroD1-based approach chosen here results in higher rates of neuronal cultures (i.e., 60–80% neurons).

To express NeuroD1 transcription factor in NSPCs, we used retrovirus-mediated genetic manipulation. We infected wild-type NSPCs isolated from the adult mouse hippocampus with virus containing NeuroD1-ERT2-IRES-GFP (NeuroD1-GFP) [18] construct and used fluorescence-activated cell sorting (FACS) to enrich for NeuroD1-GFP+ cells (Fig. 1B). Neuronal differentiation was induced by growth factor withdrawal and addition of hydroxy-tamoxifen (OH-TAM) at time point 0, here defined as day 0 (D0). We studied the metabolic profile of neuronal differentiation at 10 different time points until the 7^{th} day (D7) after differentiation induction with OH-TAM (Fig. 1B). We first confirmed that NeuroD1-GFP+ NSPCs maintained NSPC properties without TAM treatment. Indeed, NeuroD1-GFP+ NSPCs showed normal proliferative behavior compared to non-transduced cells or NSPCs transduced with control viruses (data not shown) and expressed the neural stem cell marker SRY (sex determining region Y)-box 2 (SOX2) (Fig. 1C). Next, we analyzed the rate of cell proliferation for early time points using the thymidine analogue 5-ethynyl-2'-deoxyuridine (EdU) to label cells in S-phase (Fig. 1D). We found that the proliferation rate dropped from 43±1.2% of EdU-positive cells to 24.6 ± 1.47% within the first 12 h after OH-TAM and vanished almost completely at day 1 (D1) to 1.2±0.1% cells labeled with EdU. To monitor neuronal differentiation after OH-TAM, we analyzed the expression of microtubule-associated protein 2ab (MAP2ab) as a neuronal marker and glial fibrillary acidic protein (GFAP) for astroglial cells (Fig. 1E). To determine the efficiency of neuronal differentiation with and without NeuroD1 induction, we quantified the ratio of MAP2ab and GFAP-positive cells within the differentiating NeuroD1-GFP+ NSPC population with and without OH-TAM. As expected, the majority of differentiating NSPCs where NeuroD1 expression was induced expressed MAP2ab (63.0±3.5%) with only a subset of cells expressing the glial marker GFAP (3.0±1.1%). In contrast, 63.7±3.5% of cells were GFAP-positive in control conditions without OH-TAM and only 35.4±2.5% of cells expressed MAP2ab marker.

After confirming the NeuroD1-based system of neuronal differentiation, we next analyzed the metabolic profile of proliferating NSPCs and their progeny using MS. Data analyses of metabolomics showed that there is a major metabolic shift occurring during the initial steps of cell cycle exit of NSPCs and induction of neuronal differentiation (Fig. 1F and Table S1). Subsequent principal component analyses (PCA) revealed that the largest metabolic changes occur between D1 vs. day 2 (D2) and D2 vs. day 3 (D3) (Fig. 1G). After D3 the metabolic profile did not change significantly, suggesting that the metabolic switch occurs rather quickly during the early stages of neuronal differentiation.

Our observation suggests that metabolism changes quickly with the onset of a neuronal phenotype. Clearly, the exit from cell cycle that occurs initially with functional NeuroD1 overexpression may also contribute to these changes. However, our data showing that the vast majority of NSPCs stop proliferating within the first 24 h (D1) after the addition of OH-TAM suggest that proliferation per se is not the major contributing factor to altered metabolism but that indeed the induction of neuronal differentiation leads to strong metabolic changes between D1 and D3 upon OH-TAM addition.

The data described here show that one of the most highly enriched pathways with neuronal differentiation is related to bile acid synthesis (Fig. 1H and Table S2). This is a

surprise even though recent data suggest that the brain is capable of generating bile acids [19]. Supporting this, it was previously found that one of the alternative bile acid enzyme Cyp27a1 is highly enriched in immature neurons expressing doublecortin compared to SOX2-expressing NSCs [20] [21]. Future studies will need to characterize the details and significance of metabolic changes during the course of neuronal differentiation of hippocampal NSPCs and compare these changes to metabolic adaptations described in other somatic cells in the course of cellular differentiation [22] [23] [24] [25].

For future experiments, it will be helpful to further enhance the neuronal purity of the NeuroD1-based differentiation system in cell culture. The fact that GFAP-expressing cells were never observed to be positive for GFP (data not shown) suggests that our FACS NSPC population was not 100% GFP+. There are several possibilities to improve the purity of GFP+ NSPCs. First, one could apply more stringent FACS criteria; second, NeuroD1 expression should be induced as soon as possible after FACS. This approach might prevent the small amount of GFP-cells that remained in cell culture even after FACS to relatively expand in the cultures. For our experiments, this strategy was only partially possible because the analyses of metabolic changes during several time points require relatively large amounts of cells.

Conclusions

In this study, we determined the metabolic profile of mouse hippocampal NSPCs and their neuronal progeny in vitro by mass spectrometry, using an inducible differentiation system. With this approach we captured the dynamic metabolic changes occurring during distinct steps of NSPC development. We show that proliferating NSPCs switch their metabolic profile very quickly within the 1st days of neuronal differentiation.

Limitations

This is a cell culture based experiment using forced expression of the proneurogenic transcription factor NeuroD1 to induce neuronal differentiation; results will need to be confirmed in vivo.

Additional Information

Methods

Virus production

Retroviruses were produced as previously described [18]. In summary, the Lipofectamine 2000 kit (Invitrogen) was used to transfect human embryonic kidney cells (HEK 293T) with retroviral constructs. The virus was collected 2 days after transfection by filtering the supernatant through 0.22 µm filter top and subsequent centrifugation at 19'4000 rpm/4℃ for 2 h. Viral pellet was resuspended with 4 ml PBS and spun down with 20% sucrose cushion at 20,500 rpm/4℃ for 2 h. The final viral pellet was resuspended in 40 µl PBS.

Cell culture

Wild-type (wt) mouse hippocampal NSPCs were isolated from adult mice (6–8 weeks old) as previously described [26]. Proliferating NSPCs were cultured as a monolayer with 37℃/5% CO_2 in DMEM/F-12 (Glutamax) media supplemented with N_2 (Invitrogen), antibiotics (penicillin-streptomycin-fungizone; Invitrogen), Heparin (5 µg/ml; Sigma), human EGF (20 ng/ml; PeproTech) and human basic FGF-2 (20 ng/ml; PeproTech). Media was changed every 2 days. For neuronal differentiation, media without growth factors was used (DMEM/F-12, N_2, PSF, and heparin). For the viral infection, approximately 50,000 wt adult hippocampal NSPCs were plated on coated Poly-L-ornithine (10 µg/ml; Sigma) and Laminin (5 µg/ml; Invitrogen) 12 well plates in proliferation medium. 24 h after plating, cells were infected with 1–2 µl NeuroD1-ERT2-IRES-GFP retrovirus.

FACS

NeuroD1-ERT2-IRES-GFP virus-infected NSPCs were spun down at 300 *g* for 5 min and the cell pellet was trypsinized using 0.05% trypsin in Versene for 5 min at 37℃. Afterwards a double volume of ovumucoid trypsin inhibitor mix was added for 5 min at room

temperature. Cells were resuspended with 5 ml of media and spun down at 120 *g* for 5 min. Final cell pellet was resuspended in 1 ml 1 mM EDTA in PBS or DPBS and stored on ice prior to sorting. FACS for NeuroD1-ERT2-IRES-GFP+ (NeuroD1-GFP+) cells was performed using the BD FACS Aria III Cell Sorter. For negative control/background autofluorescence, wild-type hippocampal NSPCs were used.

NeuroD1-induced neuronal differentiation

NeuroD1-induced neuronal differentiation was optimized from a previously established protocol to enable in vitro differentiation of pure neuronal cultures [18]. Proliferating NeuroD1ERT2-expressing GFP+ cells were trypsinized as described before and in parallel plated on coated (Poly-L-Lysine, 10 µg/ml and LAM) 6 well plates for metabolome analysis (330,000 cells/well in triplicates) and on coated 12 well plates (130,000 cells/well in triplicates) for the corresponding immunocytochemistry analyses. 2 days after cell plating, proliferating media was replaced with differentiating media (no growth factors) and 0.5 µM OH-TAM (Sigma; dissolved in 100% EtOH) was added. Addition of OH-TAM was defined as differentiation start (D0). Differentiation media was exchanged after 3 days. Cells were collected for metabolite extraction or in parallel for immunocytochemistry after the following time points: 6 h, 12 h, 1 day (D1), 2 days (D2), 3 days (D3), 4 days (D4), 5 days (D5), 6 days (D6) and 7 days (D7). To measure the proliferation rate during neuronal differentiation, cells on 12 well plates were pulsed with 10 mM EdU (Clik-it EdU Imaging kit; Life Technologies) for 1 h at 37℃ prior to fixation.

Immunocytochemistry

At every given time point, cells were fixed with pre-warmed (37℃) 4% paraformaldehyde (PFA) for 15 min at room temperature. Fixed plates were stored in PBS at 4℃ until immunocytochemistry was performed. Cells were treated with blocking and permeabilization buffer containing 3% donkey serum and 0.25% Triton X-100 in TBS for 30 min at room temperature. Cells were incubated with primary antibodies in blocking/permeabilization buffer overnight at 4℃. The following primary antibodies were used: goat α-SOX2 (1:200; Santa Cruz Biotechnology), rabbit α-GFAP (1:500; DAKO), mouse α-MAP2ab (1:500; Sigma). All secondary antibodies were applied for 1.5 h at room temperature in blocking/permeabilization buffer with the dilution 1:250 (Jackson Laboratories). Cell nuclei were detected with 4-6-diamidino-2-phenylindole (DAPI, 1:5000; Sigma). To analyze the cell proliferation rate, Click-it EdU Imaging kit was used according to the manufacturer's instructions.

Image analysis

Images were taken on a Zeiss Observer Z1 microscope. To analyze proliferation rate 12 h and 1 day (D1) after differentiation start, we quantified EdU and DAPI-stained nuclei. Both stained nuclei were automatically counted by self-written Fiji macro program. Number of EdU-positive DAPI nuclei was compared to EdU-negative DAPI nuclei to calculate the proliferation rate. Statistical analysis was performed using Prism6. Ordinary one way ANOVA test was performed, followed by Turkey's multiple comparisons test, p <0.0001, n= 3, SEM shown.

Quantification of neuronal and astroglial progeny with and without NeuroD1 induction

We plated 60,000 NeuroD1-GFP+ hippocampal NSPCs cells/well for each condition on glass coverslips coated with Poly-L-ornithine (50 µg/ml) and LAM (5 µg/ml) in proliferating media (DMEM/F-12 supplemented with N_2, heparin and growth factors as previously described). After 24 h, we changed the media to differentiation media (DMEM/F-12 supplemented with N_2, heparin but no growth factors) and cells were treated either with EtOH or OH-TAM (0.5 µM; SIGMA) for 2 days. During the whole differentiation process, cells were kept in differentiation media. After 7 days of differentiation, cells were fixed and stained with DAPI, anti-MAP2ab and anti-GFAP antibodies as previously described. Confocal images were taken on Olympus microscope. 5 images per well were taken. To quantify the amount of cells expressing MAP2ab and GFAP markers, we used self-written FiJi macro: a Z-stack was created with MAX intensity for all images. First, we counted DAPI particles by using the following functions: find edges, make binary, fill holes, watershed and analyze particles size 30–300, circularity 0.40–1.00. Then we analyzed MAP2ab and GFAP expression by setting a threshold and converting it to a mask. Threshold was adjusted for each condition to yield a better separation of MAP2ab and

GFAP-positive cells and to eliminate any overlap in the channels. This mask was selected and laid over the DAPI particles. Then all DAPI particles overlaying the GFAP or MAP2ab mask were counted using the analyze particle function with size 30–300, circularity 0.30–1.00. The counted particles for MAP2ab and GFAP were divided by the DAPI counted particles to get the ratio of MAP2ab and GFAP-positive cells per condition. In total, 3,197 DAPI+ cells were counted for ETOH condition and 2249 DAPI+ for OH-TAM condition.

Metabolite extraction

At every given time point, cells were washed with 75 mM ammonium carbonate (Sigma) pH 7.4 and snap-frozen on the plates with liquid nitrogen. Metabolites were extracted by treating the snap-frozen plates with hot extraction solution (70% EtOH) on heating block (75℃). The plate was re-extracted with hot extraction solution 2 more times, allowing for a high recovery rate. Note that the extraction efficiency is irrelevant for the analyses performed here given that we did not perform quantitative analyses but a qualitative comparison between conditions. Hence, full recovery is not a precondition to detect difference in metabolites across groups. Supernatant containing metabolites from all 3 extractions was pooled, spun down, and stored at -80℃ until mass spectrometry measurements.

Mass spectrometry measurements and data analyses

For non-targeted metabolite profiling, metabolite samples were analyzed by flow injection analysis on an FIA Agilent Q-TOF 6550 QTOF instrument (Agilent, Santa Clara, CA) in negative mode at 4 GHz, high resolution in a m/z range of 50–1000 [27]. A 60:40 mixture of isopropanol:water supplemented with NH_4F at pH 9.0, as well as 10 nM hexakis (1H, 1H, 3H-tetrafluoropropoxy) phosphazine and 80 nM taurochloric acid for online mass calibration. Ions were putatively annotated to metabolites based on exact mass using a tolerance of 0.001 Da and the KEGG hsa database following the procedure described in [27]. Notably, this procedure does not allow distinguishing metabolites with same molecular formula or weight. For full disclosure, all putative matches are reported in Table S1. All data analyses were performed using Matlab (The Mathworks, Natick).

Supplementary Material

Please see https://sciencematters.io/articles/201603000016.

Funding Statement

Supported by EMBO Young Investigator program and Swiss National Science Foundation (SNSF) consolidator grant (BSCGIo_157859) and an SNSF project grant (31003A_-156943) (all to SJ).

Acknowledgements

We thank M. Knobloch for experimental advice and critical comments on the manuscript. We also thank the ZMB imaging facility and flow cytometry facility of the University of Zurich. M.H. and S.J. are members of the Zurich Neuroscience Center (ZNZ) of the University of Zurich and ETH Zurich. The authors declare no competing financial interests.

Ethics Statement

Not applicable.

Citations

[1] H. Georg Kuhn, Heather Dickinson-Anson, and Fred H. Gage. "Neurogenesis in the dentate gyrus of the adult rat: age-related decrease of neuronal progenitor proliferation". In: *Journal of Neuroscience* 16 (1996), pp. 2027–2033.

[2] Fred H. Gage. "Mammalian Neural Stem Cells". In: *Science* 287.5457 (Feb. 2000), pp. 1433–1438. DOI: 10.1126/science.287.5457.1433. URL: http://dx.doi.org/10.1126/science.287.5457.1433.

[3] Kirsty L. Spalding et al. "Dynamics of Hippocampal Neurogenesis in Adult Humans". In: *Cell* 153.6 (June 2013), pp. 1219–1227. DOI: 10.1016/j.cell.2013.05.002. URL: http://dx.doi.org/10.1016/j.cell.2013.05.002.

[4] E. Drapeau et al. "Spatial memory performances of aged rats in the water maze predict levels of hippocampal neurogenesis". In: *Proceedings of the National Academy of Sciences* 100.24 (Nov. 2003), pp. 14385–14390. DOI: 10.1073/pnas.2334169100. URL: http://dx.doi.org/10.1073/pnas.2334169100.

[5] Kimberly M. Christian, Hongjun Song, and Guo-li Ming. "Functions and Dysfunctions of Adult Hippocampal Neurogenesis". In: *Annual Review of Neuroscience* 37.1 (July 2014), pp. 243–262. DOI: 10.1146/annurev-neuro-071013-014134. URL: http://dx.doi.org/10.1146/annurev-neuro-071013-014134.

[6] Jack M. Parent et al. "Dentate Granule Cell Neurogenesis Is Increased by Seizures and Contributes to Aberrant Network Reorganization in the Adult Rat Hippocampus". In: *Journal of Neuroscience* 17 (1997), pp. 3727–3738.

[7] Luca Santarelli et al. "Requirement of Hippocampal Neurogenesis for the Behavioral Effects of Antidepressants". In: *Science* 301.5634 (Aug. 2003), pp. 805–809. DOI: 10.1126/science.1083328. URL: http://dx.doi.org/10.1126/science.1083328.

[8] Nataliya E. Chorna et al. "Fatty Acid Synthase as a Factor Required for Exercise-Induced Cognitive Enhancement and Dentate Gyrus Cellular Proliferation". In: *PLOS ONE* 8.11 (Nov. 2013), e77845. DOI: 10.1371/journal.pone.0077845. URL: http://dx.doi.org/10.1371/journal.pone.0077845.

[9] Marlen Knobloch et al. "Metabolic control of adult neural stem cell activity by Fasn-dependent lipogenesis". In: *Nature* 493.7431 (Dec. 2012), pp. 226–230. DOI: 10.1038/nature11689. URL: http://dx.doi.org/10.1038/nature11689.

[10] Sophia Y. Lunt and Matthew G. Vander Heiden. "Aerobic Glycolysis: Meeting the Metabolic Requirements of Cell Proliferation". In: *Annual Review of Cell and Developmental Biology* 27.1 (Nov. 2011), pp. 441–464. DOI: 10.1146/annurev-cellbio-092910-154237. URL: http://dx.doi.org/10.1146/annurev-cellbio-092910-154237.

[11] Clifford D.L. Folmes et al. "Metabolic Plasticity in Stem Cell Homeostasis and Differentiation". In: *Cell Stem Cell* 11.5 (Nov. 2012), pp. 596–606. DOI: 10.1016/j.stem.2012.10.002. URL: http://dx.doi.org/10.1016/j.stem.2012.10.002.

[12] Keisuke Ito and Toshio Suda. "Metabolic requirements for the maintenance of self-renewing stem cells". In: *Nature Reviews Molecular Cell Biology* 15.4 (Mar. 2014), pp. 243–256. DOI: 10.1038/nrm3772. URL: http://dx.doi.org/10.1038/nrm3772.

[13] Rachel David. "Stem cells: LKB1 maintains the balance". In: *Nature Reviews Molecular Cell Biology* 12.1 (Dec. 2010), pp. 4–5. DOI: 10.1038/nrm3032. URL: http://dx.doi.org/10.1038/nrm3032.

[14] Keisuke Ito et al. "A PML–PPAR-δ pathway for fatty acid oxidation regulates hematopoietic stem cell maintenance". In: *Nature Medicine* 18.9 (Aug. 2012), pp. 1350–1358. DOI: 10.1038/nm.2882. URL: http://dx.doi.org/10.1038/nm.2882.

[15] Arieh Moussaieff et al. "Glycolysis-Mediated Changes in Acetyl-CoA and Histone Acetylation Control the Early Differentiation of Embryonic Stem Cells". In: *Cell Metabolism* 21.3 (Mar. 2015), pp. 392–402. DOI: 10.1016/j.cmet.2015.02.002. URL: http://dx.doi.org/10.1016/j.cmet.2015.02.002.

[16] Hideshi Kawakami et al. "Cloning and Expression of a Rat Brain Basic Helix–Loop–Helix Factor". In: *Biochemical and Biophysical Research Communications* 221.1 (Apr. 1996), pp. 199–204. DOI: 10.1006/bbrc.1996.0569. URL: http://dx.doi.org/10.1006/bbrc.1996.0569.

[17] Zhengliang Gao et al. "Neurod1 is essential for the survival and maturation of adult-born neurons". In: *Nature Neuroscience* 12.9 (Aug. 2009), pp. 1090–1092. DOI: 10.1038/nn.2385. URL: http://dx.doi.org/10.1038/nn.2385.

[18] Simon M.G. Braun, Raquel A.C. Machado, and Sebastian Jessberger. "Temporal Control of Retroviral Transgene Expression in Newborn Cells in the Adult Brain". In: *Stem Cell Reports* 1.2 (Aug. 2013), pp. 114–122. DOI: 10.1016/j.stemcr.2013.06.003. URL: http://dx.doi.org/10.1016/j.stemcr.2013.06.003.

[19] Matthew Quinn and Sharon DeMorrow. "Bile in the Brain? A Role for Bile Acids in the Central Nervous System". In: *Journal of Cell Science and Therapy* 03.07 (2013). DOI: 10.4172/2157-7013.1000e113. URL: http://dx.doi.org/10.4172/2157-7013.1000e113.

[20] O. Bracko et al. "Gene Expression Profiling of Neural Stem Cells and Their Neuronal Progeny Reveals IGF2 as a Regulator of Adult Hippocampal Neurogenesis". In: *Journal of Neuroscience* 32.10 (Mar. 2012), pp. 3376–3387. DOI: 10.1523/jneurosci.4248-11.2012. URL: http://dx.doi.org/10.1523/jneurosci.4248-11.2012.

[21] Z. Ali et al. "On the regulatory role of side-chain hydroxylated oxysterols in the brain. Lessons from CYP27A1 transgenic and Cyp27a1-/- mice". In: *The Journal of Lipid Research* 54.4 (Jan. 2013), pp. 1033–1043. DOI: 10.1194/jlr.m034124. URL: http://dx.doi.org/10.1194/jlr.m034124.

[22] Girish Pattappa et al. "The metabolism of human mesenchymal stem cells during proliferation and differentiation". In: *Journal of Cellular Physiology* 226.10 (July 2011), pp. 2562–2570. DOI: 10.1002/jcp.22605. URL: http://dx.doi.org/10.1002/jcp.22605.

[23] Keiyo Takubo et al. "Regulation of Glycolysis by Pdk Functions as a Metabolic Checkpoint for Cell Cycle Quiescence in Hematopoietic Stem Cells". In: *Cell Stem Cell* 12.1 (Jan. 2013), pp. 49–61. DOI: 10.1016/j.stem.2012.10.011. URL: http://dx.doi.org/10.1016/j.stem.2012.10.011.

[24] Anna Halama et al. "Metabolic signatures differentiate ovarian from colon cancer cell lines". In: *Journal of Translational Medicine* 13.1 (July 2015). DOI: 10.1186/s12967-015-0576-z. URL: http://dx.doi.org/10.1186/s12967-015-0576-z.

[25] Hasbullah Daud et al. "Metabolic profiling of hematopoietic stem and progenitor cells during proliferation and differentiation into red blood cells". In: *New Biotechnology* 33.1 (Jan. 2016), pp. 179–186. DOI: 10.1016/j.nbt.2015.05.002. URL: http://dx.doi.org/10.1016/j.nbt.2015.05.002.

[26] D. L. Moore et al. "A mechanism for the segregation of age in mammalian neural stem cells". In: *Science* 349.6254 (Sept. 2015), pp. 1334–1338. DOI: 10.1126/science.aac9868. URL: http://dx.doi.org/10.1126/science.aac9868.

[27] Tobias Fuhrer et al. "High-Throughput, Accurate Mass Metabolome Profiling of Cellular Extracts by Flow Injection–Time-of-Flight Mass Spectrometry". In: *Analytical Chemistry* 83.18 (Sept. 2011), pp. 7074–7080. DOI: 10.1021/ac201267k. URL: http://dx.doi.org/10.1021/ac201267k.